

MOVING OBSTACLE DETECTION AND AVOIDANCE FOR UNMANNED  
GROUND VEHICLE

by

GANGADHAR RAJASHEKARAI AH

Presented to the Faculty of the Graduate School of  
The University of Texas at Arlington in Partial Fulfillment  
of the Requirements  
for the Degree of

MASTER OF SCIENCE IN MECHANICAL ENGINEERING

THE UNIVERSITY OF TEXAS AT ARLINGTON

December 2014

Copyright © by Gangadhar Rajashekaraiiah 2014  
All Rights Reserved

Dedicated to my family and friends

## ACKNOWLEDGEMENTS

First, I would like to thank my supervising professor Dr. Atilla Dogan for his continuous guidance and support over the years of my research at University of Texas Arlington. During this tenure under Dr. Dogan I learnt a lot on problem solving techniques, he was always there to help and encourage me throughout my thesis work. I could not have imagined a better guide and advisor for my masters thesis. I am really grateful to Dr. Dogan for providing me an opportunity to work under him.

I convey my regards to Dr. Huff as well as Dr. Subbarao for taking time to be on my thesis committee. I am grateful to Dr. Huff for providing the necessary hardware required for carrying out the real time experiments whenever required.

Beside this, I would also like to thank Dr. Sevil and Onur for answering all my queries with patience. It would have been really difficult for me to understand many concepts involved in my research without their help.

Lastly, I am grateful to my parents, teachers, friends for their everlasting support and inspiration, without them it would have been impossible for me to complete this assignment.

November 24, 2014

## ABSTRACT

# MOVING OBSTACLE DETECTION AND AVOIDANCE FOR UNMANNED GROUND VEHICLE

Gangadhar Rajashekaraiyah, M.S.

The University of Texas at Arlington, 2014

Supervising Professors: Atilla Dogan

This thesis presents the development and implementation of an autonomous obstacle avoidance algorithm for UGV (Unmanned Ground Vehicle). The research improves the prior work by enhancing the obstacle avoidance capability to handle moving obstacle as well as stationary obstacles. A mathematical representation of the area of operation with obstacles is formulated by PTEM (Probabilistic Threat Exposure Map). The PTEM quantifies the risk in being at a position in an area with different types of threat. Threat in this context means UGV getting close to or running into stationary and moving obstacles. A LRF (Laser Range Finder) sensor mounted on the UGV is used to collect information about the obstacles in the area. LRF readings are used to construct the PTEM. A guidance algorithm processes the PTEM and generates the guidance (speed and heading) commands to steer the UGV to assigned waypoints while avoiding obstacles. The main contribution of this research work is to update the PTEM continuously as new LRF reading are obtained. With this approach, no change is needed in the guidance algorithm since the PTEM will have representation of the obstacles at any given time and the guidance algo-

rithm processes the updated PTEM. The improved PTEM construction algorithm is implemented in a MATLAB/Simulink simulation environment that includes models of the UGV, LRF, all the sensors and actuators needed for the control of the UGV. The performance of the algorithm is also demonstrated in realtime experiments with an actual UGV system.

## TABLE OF CONTENTS

ACKNOWLEDGEMENTS . . . . .	iv
ABSTRACT . . . . .	v
LIST OF FIGURES . . . . .	x
1. Introduction . . . . .	1
1.1 Research Motivation . . . . .	1
1.2 Application of Unmanned Vehicle Systems . . . . .	2
1.3 Thesis Objective . . . . .	2
1.4 Thesis Organization and Contribution . . . . .	3
1.4.1 Thesis Organization . . . . .	3
1.4.2 Contribution . . . . .	4
2. Literature Review . . . . .	5
2.1 Introduction . . . . .	5
2.2 Sensors . . . . .	5
2.3 Moving Obstacle Avoidance Techniques . . . . .	6
2.4 Simulation . . . . .	7
2.5 Real Time Implementation . . . . .	7
3. Unmanned Ground Vehicle (UGV) . . . . .	9
3.1 Description . . . . .	9
3.2 Hardware . . . . .	10
3.2.1 Laser Range Finder (LRF) . . . . .	10
3.2.2 Rotary Encoders . . . . .	11
3.2.3 MPC 555 Microcontroller . . . . .	11

3.3	Model . . . . .	12
3.3.1	UGV Simulink Model . . . . .	12
3.3.2	Kinematic Equations for UGV . . . . .	14
4.	Obstacle Avoidance Algorithm . . . . .	15
4.1	PTEM Definition . . . . .	15
4.2	PTEM Construction . . . . .	16
4.2.1	Clustering of LaserRangeFinder Data . . . . .	16
4.2.2	Cumulative Clustering Algorithm . . . . .	17
4.2.3	Single Scan Clustering Algorithm . . . . .	18
4.2.4	Case 1 . . . . .	19
4.2.5	Case 2 . . . . .	20
4.3	Determining PTEM Variables . . . . .	21
4.4	Virtual Target . . . . .	22
4.5	Guidance Algorithm . . . . .	22
5.	Stationary Obstacle Avoidance . . . . .	24
5.1	Stationary Obstacle Avoidance Simulation Results . . . . .	24
5.1.1	Case 1 . . . . .	24
5.1.2	Case 2 . . . . .	26
5.2	Stationary Obstacle Avoidance Experimental Results . . . . .	27
5.2.1	Case 1 . . . . .	28
5.2.2	Case 2 . . . . .	30
6.	Dynamic Obstacle Avoidance . . . . .	32
6.1	Moving Obstacle Simulation Results . . . . .	32
6.1.1	Case 1 . . . . .	32
6.1.2	Case 2 . . . . .	34
6.2	Moving Obstacle Experimental Results . . . . .	36



6.2.1	Case 1 . . . . .	37
6.2.2	Case 2 . . . . .	39
6.3	Problems Observed in Experiments . . . . .	40
6.3.1	Observation 1 . . . . .	40
6.3.2	Observation 2 . . . . .	41
7.	Conclusion and Future Work . . . . .	42
7.1	Conclusion . . . . .	42
7.2	Future Work . . . . .	43
	REFERENCES . . . . .	44
	BIOGRAPHICAL STATEMENT . . . . .	49

## LIST OF FIGURES

Figure	Page
3.1 Unmanned Ground Vehicle . . . . .	9
3.2 Laser Range Finder . . . . .	10
3.3 Encoder . . . . .	11
3.4 MPC 555 Micro-controller . . . . .	12
3.5 Simulink Model . . . . .	13
4.1 Clustering Data Points . . . . .	17
4.2 Single Scan Clustering Algorithm . . . . .	19
4.3 Cumulative Clustering Algorithm . . . . .	19
4.4 Single Scan Clustering Algorithm . . . . .	20
5.1 Trajectory of UGV avoiding thin stationary obstacle . . . . .	24
5.2 PTEM variables comparison b/w Cumulative and single scan approach for stationary obstacle Case 1 . . . . .	25
5.3 Trajectory of UGV avoiding stationary obstacle (Cone) . . . . .	26
5.4 PTEM variables comparison b/w Cumulative and single scan approach for stationary obstacle Case 2 . . . . .	27
5.5 Stationary Obstacles . . . . .	28
5.6 Real Time UGV Trajectory avoiding stationary thin obstacle . . . . .	28
5.7 PTEM variables comparison b/w Cumulative and single scan approach for stationary obstacle Case 1 . . . . .	29
5.8 UGV Trajectory in Real Time avoiding stationary cone obstacle . . . . .	30

5.9	PTEM variables comparison b/w Cumulative and single scan approach for stationary obstacle Case 2 . . . . .	31
6.1	Trajectory of UGV for Moving obstacle . . . . .	32
6.2	PTEM variables comparison b/w Cumulative and single scan approach for dynamic obstacle Case 1 . . . . .	33
6.3	Trajectory of UGV for Moving obstacle . . . . .	34
6.4	PTEM variables comparison b/w Cumulative and single scan approach for dynamic obstacle Case 2 . . . . .	35
6.5	Moving Obstacle . . . . .	36
6.6	Trajectory of UGV . . . . .	37
6.7	PTEM variables comparison b/w Cumulative and single scan approach for dynamic obstacle Case 1 . . . . .	37
6.8	Trajectory of UGV . . . . .	39
6.9	PTEM variables comparison b/w Cumulative and single scan approach for dynamic obstacle Case 2 . . . . .	40

## CHAPTER 1

### Introduction

This chapter explains the problem statement for the thesis research work. It also describes the motivation for carrying out this research, along with application of UVS (Unmanned Vehicle Systems) and finally gives a brief description on thesis organization.

#### 1.1 Research Motivation

UVS are used in various application nowadays ranging from automobiles, public transportation, industrial and military sector. The technological advancement has made it possible for the UVS to operate in hazardous environment without human intervention, which minimizes the risk to human life and property. The innovations in science and technology can be effectively used to build unmanned systems so that they operate autonomously. The primary requirement for autonomy depends on how fast the unmanned systems detect changes in its environment and respond to these changes efficiently [1]. A type of autonomy can be achieved by developing guidance and control algorithms that can pilot the unmanned vehicle system to their destination while avoiding all the obstacles, restricted regions coming in their way.

Unmanned systems include drones (Unmanned Aircraft), intelligent cars, underwater and water surface vehicles. In this research the main focus is on UGV (Unmanned Ground Vehicle), however the algorithms developed can potentially be implemented on the unmanned aerial vehicle platform with suitable modifications.

## 1.2 Application of Unmanned Vehicle Systems

Unmanned vehicle systems have variety of applications in the field of automotive, farming and military sectors [2]. The motivation behind Google self driving cars is to reduce accidents and traffics jams caused due to human error. Driver-less cars also enable senior citizens to retain their independence. Self driving cars have already caught attention of many companies. Many of the semi autonomous features like automatic braking systems when approaching obstacles and cruise controller are already in use. Congested ports are using fleets of transport vehicles which can coordinate among themselves to quickly transport the cargo. In a very near future one can see driver-less tractor ploughing fields. UVS has many roles [3, 4] to play in the military operations. They can deliver supplies and ammunition to the troops on ground as well as carry out surveillance and attack fixed targets on the ground. UGV can also be used for deactivating the unexploded bombs.

## 1.3 Thesis Objective

The obstacle avoidance capacity of UGV is enhanced by building upon the prior work [5] that already has stationary obstacle avoidance capability. **The main objective of this research is to modify PTEM construction algorithm so that the UGV can avoid both stationary as well as the moving obstacles. The modified PTEM construction algorithm must enable the UGV to navigate to the specified waypoints while avoiding the moving obstacle in its path. Moving obstacles are handled by representing them in PTEM at any given time.** Prior guidance algorithm can enable the UGV used to successfully avoid stationary obstacles but the PTEM construction algorithm did not consider the possibility that the obstacles detected may not be stationary. As a result, all

the obstacle information is retained within the PTEM at the positions they are first detected. This resulted in restricted regions represented within the PTEM growing inadvertently if an obstacle is moving and thus the UGV finding itself within the restricted region even though there is no obstacle that large.

The objective of this research is accomplished by carrying out the following steps:

1. Identifying the problem associated with the moving obstacle
2. Modifying the PTEM construction algorithm to handle to moving obstacles.
3. Running the simulation to see whether the results meet the required objective.
4. Implement the new algorithm on the actual UGV for real-time experiment and validation.

## 1.4 Thesis Organization and Contribution

### 1.4.1 Thesis Organization

Chapter 2 provides a literature review of the previous work done in this field. This chapter explains the various types of sensors and algorithms used for obstacle avoidance and navigation of UGV. It also gives a brief description on real time implementation techniques and the hardware associated with it.

Chapter 3 describes the platform used for realtime implementation of obstacle avoidance algorithm and the hardware associated with this. It also explains the simulink model associated with this platform.

Chapter 4 gives a brief description of the cumulative clustering and single scan clustering algorithm. It explains the PTEM construction procedure and its integration within the obstacle avoidance and waypoint navigation of the UGV.

Chapter 5 describes the simulation and experimental results of stationary obstacle avoidance and waypoint navigation with the prior PTEM construction and new single scan clustering algorithm.

Chapter 6 presents how the new PTEM construction algorithm improves the performance in avoiding the moving obstacles. Simulation and experimental results of moving obstacle avoidance and waypoint navigation with the prior PTEM construction and new single scan clustering algorithm are presented.

Chapter 7 gives a summary of the findings of this research work and details the conclusions reached. It also discusses several ideas for future work to further improve the obstacle avoidance performance with more diverse and complicated obstacles and obstacle motions.

#### 1.4.2 Contribution

The main contribution of this research work is to enable the existing UGV platform to avoid moving obstacles as well as stationary obstacles. The prior PTEM construction algorithm made the assumption of stationary obstacles and thus treat the LRF (Laser Range Finder) readings as persistent obstacle information. This led to prohibitively large restricted area representations within the PTEM representation when obstacles happen to be moving. This research effort removes the stationary obstacle assumptions and builds PTEM based on the most recent LRF scan regardless of the previous LRF readings within the area covered by the previous LRF scan.

## CHAPTER 2

### Literature Review

#### 2.1 Introduction

A challenging aspect in vehicle autonomy is the navigation of the system in an environment filled with uncertainties. The autonomous vehicle should avoid all the obstacles in its path and reach the destination. In order to navigate towards its assigned waypoint, vehicle should sense its surrounding for obstacles. One can use various sensors for detecting obstacles. Some of the commonly used sensors in the field of autonomous vehicles are discussed in this chapter. Similarly different approaches can be used for collision avoidance algorithms, some of which are discussed below. Not all algorithms developed for obstacle avoidance are implemented in real time. In addition to work done in simulation, a brief discussion is added on the realtime implementation of obstacle detection and avoidance algorithms.

#### 2.2 Sensors

Sensors are chosen based on the features essential to operate the autonomous system. The primary requirements [1] for autonomous navigation is to sense changes in vehicle's environment and react to it without human intervention. Hence sensors are one of the vital components in obstacle avoidance and navigation of unmanned vehicle systems. Sensors must have large enough sensing range and the sampling speed should be fast enough to provide the real time information in the dynamic environment. There are wide variety of sensors used in autonomous vehicle systems, some of which are discussed below.



LRF (Laser Range Finder) [1,6–9] is one of the commonly used sensors for obstacle detection. Some of the commonly used LRF in obstacle avoidance are discussed below. LRF known as [6], SICK LMS 200 provides distance measurements, over a 180 degree area, up to 80 meters away. SICK LD-OEM 1000 LRF [10] scans the full 360 degree. The scanning frequency can be varied from 5 Hz to 15 Hz with an angular resolution of 0.125 to 1.5 degrees. Ultrasonic sensors [11–15] are also widely used in obstacle avoidance and navigation of autonomous vehicles because of low cost, low energy usage, high directivity as well as its ability to measure long distances accurately [13].

Nowadays vision based systems are used extensively [4, 10, 16–19] since they can acquire the information of whole environment. Vision sensors provide 3D data of complex objects. However due to huge computation quantity, high capability devices are required to process the information. There are situations where vision sensors cannot provide accurate range information such as during poor lighting conditions. A robotic platform known as Safobot [6] uses visual sensor Logitech web camera to track humans. It has a fixed view and can acquire 320×240 color images.

### 2.3 Moving Obstacle Avoidance Techniques

The autonomous vehicles should be able to represent its surrounding environment and plan a path to its destination. A collision free path has to be built and laid out to succeed in mission. Some of the moving obstacle avoidance techniques are discussed below.

Potential field methods has been used [6, 20–22] in obstacle avoidance for mobile robots. The method is very attractive because of its simplicity. In this approach the obstacles exert repulsive forces on the robot while the target employs attractive forces. The resultant force regulates the speed and path to be followed by the robot.

However there are a few disadvantages [22] that are bound to surface in actual implementation. Some of the limitations of Potential field methods are [22], trap-situation which occurs when robot enter U-shaped obstacle, no passage between two closely spaced obstacles and one of the most significant limitations of potential field method is their tendency to cause unstable motion in the presence of obstacles. In a similar way robot experience oscillation when it passes through a narrow passage because of the repulsive forces coming from walls.

Probabilistic inference [23–26] is used in mobile robots for avoiding moving obstacle by planning their paths. Whenever there is uncertainty in the information probabilistic methods are mostly used. Probabilistic methods have certain advantages [25] over the other techniques such as "well established theoretical frame work , ability to accommodate non deterministic nature of problem and using the probability density function one can specify threat level of an area".

## 2.4 Simulation

Simulation demonstrates the effectiveness of the algorithms developed for obstacle avoidance. Almost all the algorithms developed are tested in simulation environment. Refs. [27] demonstrate the performance of obstacle avoidance algorithms using numerical simulations. The results from the numerical simulation environment show the robot avoiding moving obstacles. Simulation was performed in matlab to investigate whether the algorithm proposed is effective [23].

## 2.5 Real Time Implementation

Real time implementation of obstacle avoidance algorithms is important to validate their performance in actual conditions. Algorithms developed are rarely tested in

real time. Refs. [1,28,29] discuss the real-time algorithms and the platforms involved involved in real-time implementation. A few platforms are briefly explained below just to give an insight about the hardware associated with testing the algorithms.

The mobile robot in [27] consists of two 12V batteries which drives the left and right wheel of the robot. Each wheel is equipped with a DC motor. The system consists of Pentium-IV 2.2 GHz single board computer with a PCI interface (peripheral component interface). Similarly, Ref. [6] has two independent tracks for robotic mobility where each of the track has the capability to move the robot on its own. RS-232 signal are sent from the computer that controls the motion of the robot by sending the commands to the track motors. Robot mobility phase is activated if an obstacle is detected. Experiment results have shown that the robot avoids the obstacle successfully and track the moving object.

## CHAPTER 3

### Unmanned Ground Vehicle (UGV)

#### 3.1 Description

UGV platform used in this research [1, 5] is 27 inch  $\times$  15 inch tracked skid-steered platform as shown in the Fig. 3.1. Platform has two conventional DC motors and H-bridges are included to support the backward motion of UGV. PWM (Pulse Width Modulation) signals sent by the controller drives the platform. Encoders are directly attached to shafts which measure the angular displacements of the drive sprockets. Two 12 V, 10.5 Ah batteries are used to power the on-board sensors, micro-controller and to drive motors. Total weight of the platform is under 34 pounds.

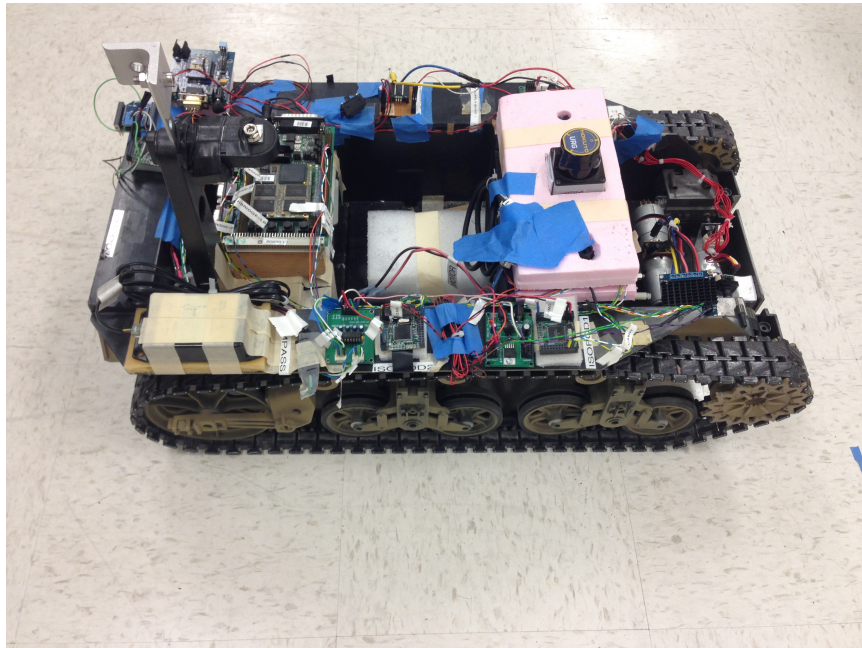


Figure 3.1. Unmanned Ground Vehicle.

## 3.2 Hardware

### 3.2.1 Laser Range Finder (LRF)

LRF used in this research is Hokuyo URG-04LX [1, 5] as shown in the Fig. 3.2. It has a sense range of 4 meters with an accuracy  $\pm 20$  mm and a 240 degree sweep angle. Angular resolution of LRF is 0.36 degrees with a scanning time of 100 milliseconds per scan. LRF is connected to PlugAPod<sup>R</sup> through a serial cable. PlugAPod<sup>R</sup> controller first initiates the scan and the LRFs return 769 two byte values that are encoded in a proprietary data structure. PlugAPod<sup>R</sup> parses the scanned data as angle of an obstacle point and distance to the detected obstacle point. Once the scan is complete, positions and angle information of the detected obstacle points are sent to MPC555 micro-controller for further processing via CAN network as a CAN message.



Figure 3.2. Laser Range Finder.

### 3.2.2 Rotary Encoders

Encoders are directly attached to the drive shaft of the platform. They measure angular displacement of the platform's drive sprockets. Encoder counts coming from the right and left shaft of the UGV are used to calculate the estimated velocity, heading as well as the position of the vehicle platform by dead reckoning algorithm. Each encoder has two outputs and a power supply (+5V and ground). Outputs of the encoder are connected to TPU (Timer Processing Unit) of MPC555 micro-controller.

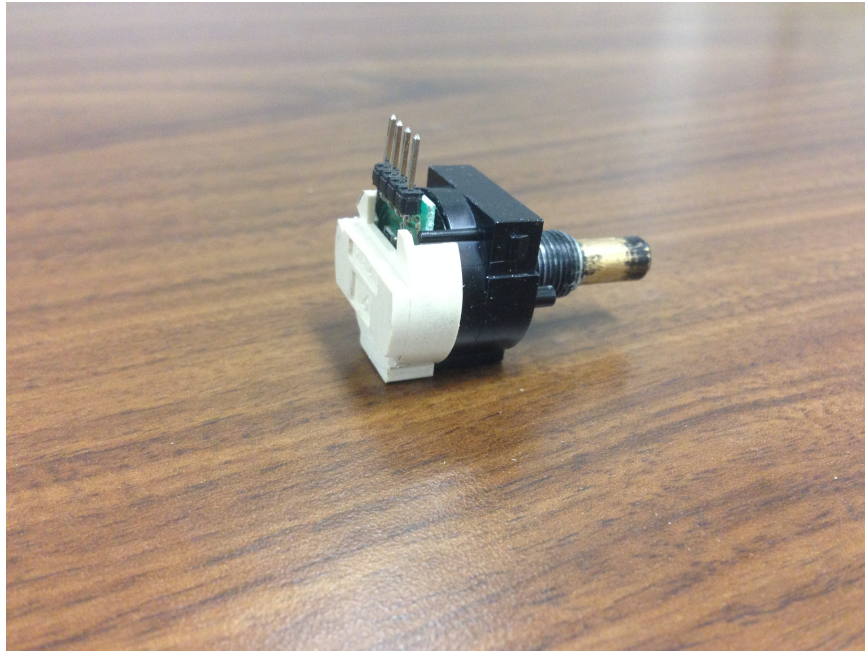


Figure 3.3. Encoder.

### 3.2.3 MPC 555 Microcontroller

The heart of vehicle controller is phyCORE-MPC555 development system, which uses Freescale 32-bit 40MHz MPC555 micro-controller [1, 5]. Micro-controller receives the information from the sensors, processes this information to construct PTEM and finally gives the heading and velocity control signals for the vehicle platform to reach

the desired waypoint. PWM signals are sent out from MPC 555 to drive the platform. Encoder readings are transmitted to MPC 555 via TPU from which the position and heading of vehicle are estimated using dead reckoning algorithm.

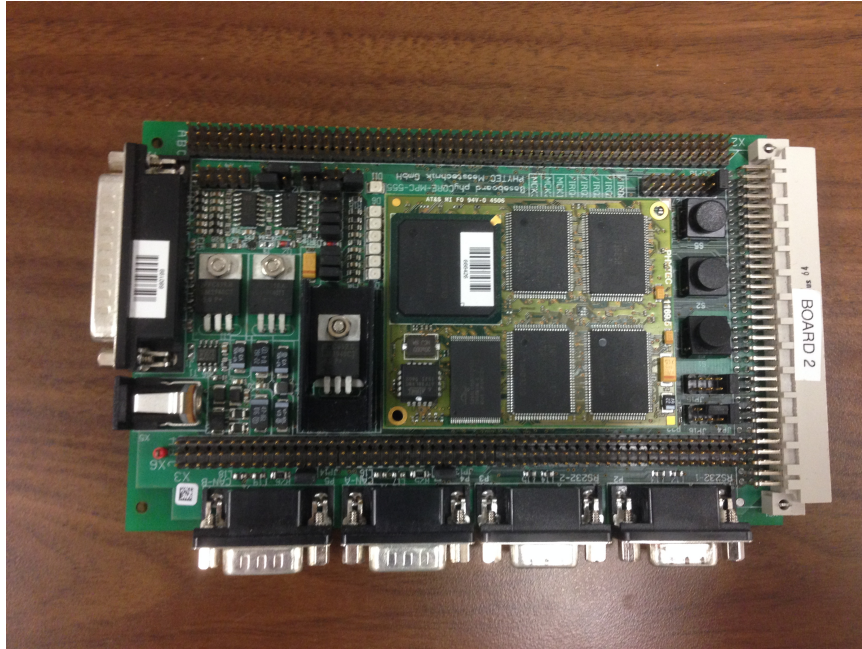


Figure 3.4. MPC 555 Micro-controller.

### 3.3 Model

#### 3.3.1 UGV Simulink Model

Fig. 3.5 shows the simulink model of the platform used in this research. Input to this model are percent duty cycles of PWM signals, which are converted into angular velocities of right and left wheel using the look up tables. The platform requires minimum of 30 percent PWM duty cycle signal to move from rest. Rate transition blocks are included since there is a transition from digital system to analog system.

A first order transfer function with a time constant of 0.1 s is included in the model to represent the powertrain dynamics. When same  $\omega_r$  and  $\omega_l$  are applied to the wheels the tank moves in a straight line, if  $\omega_r > \omega_l$  the tank makes a left turn and  $\omega_l > \omega_r$  tank makes a right turn.

The left and right angular velocities are converted to their respective encoder ticks by.

$$eCount = rNominal \times eTick \times \int \omega dt \quad (3.1)$$

where  $rNominal$  is radius of left or right wheel of the platform,  $\omega$  is angular velocities of right or left wheel and  $eTick$  represents number of ticks per meter translation of the vehicle.

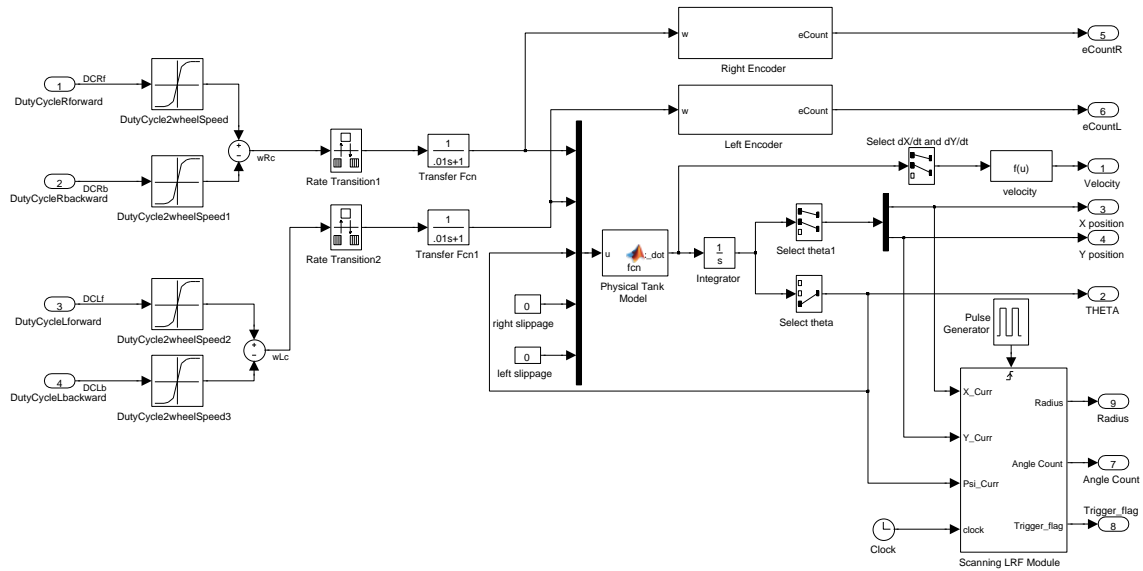


Figure 3.5. Simulink Model.



### 3.3.2 Kinematic Equations for UGV

The kinematics of the UGV relates the translational and rotational velocity of the platform to wheel speeds and orientation [5] as

$$\dot{X} = [(1 - s_r) \quad rr \quad \omega_r + (1 - s_l) \quad rl \quad \omega_l] \frac{\cos \theta}{2} \quad (3.2)$$

$$\dot{Y} = [(1 - s_r) \quad rr \quad \omega_r + (1 - s_l) \quad rl \quad \omega_l] \frac{\sin \theta}{2} \quad (3.3)$$

$$\dot{\theta} = [(1 - s_r) \quad rr \quad \omega_r - (1 - s_l) \quad rl \quad \omega_l] \frac{1}{b} \quad (3.4)$$

where  $\omega_r$  &  $\omega_l$  angular velocities of the right and left wheel,  $s_r$  &  $s_l$  are slippage constants for right and left wheel,  $rr$  &  $rl$  are radius of the right and left wheel,  $\theta$  is Heading Angle of the UGV,  $b$  is diagonal width of the vehicle,  $\dot{X}$  &  $\dot{Y}$  are velocity components in X and Y direction and  $\dot{\theta}$  is turn rate of the Tank.

The embedded matlab function in Fig. 3.5 contains the kinematic equations of the vehicle. Input to this are the angular velocities of the right and left wheel where  $rr, rl, sr, sl$  and  $b$  are the parameters. Outputs are the position and heading of the vehicle. The velocity components and heading rate are passed through an integrator to obtain the positions as well as heading of the platform.

## CHAPTER 4

### Obstacle Avoidance Algorithm

This chapter presents the components of the obstacle avoidance algorithm, particularly the construction of an obstacle map. The obstacle map is formulated using the concept of PTEM (Probabilistic Threat Exposure Map), which is processed by a guidance algorithm to steer the UGV to avoid obstacles while moving through assigned waypoints. The PTEM is constructed based on the readings from the LRF. First, the prior PTEM construction method is presented, followed by the new PTEM construction method developed in this research to handle moving obstacles. The guidance algorithm and the virtual target concept used for the guidance algorithm for waypoint navigation are also presented in this chapter.

#### 4.1 PTEM Definition

PTEM quantifies the risk in being at a position in an area with different types of threat [1,30]. "A PTEM indicates the level of exposure to risk, including getting very close or running into obstacles at given position in an area of operation". This concept defines various types of threats such as objects, locations that need to be avoided in a single framework. Once the PTEM is constructed there is no need to distinguish between the different type and size of obstacles because all the decisions are made using the PTEM map. PTEM is a continuous probabilistic map consisting the sum of multidimensional PDFs (Probability Density Functions). There are two parameters that need to be fully specified for a Gaussian PDF; the mean value specifies the concentration point (location) and the variance specifies the area of influence of

the PDF. The PTEM is defined as the sum of multiple multidimensional Gaussian PDFs as

$$f(r) = \sum_{i=1}^N \frac{1}{2\pi\sqrt{\det(K_i)}} \exp\left[-\frac{1}{2}(r - \mu_i)^T K_i^{-1}(r - \mu_i)\right] \quad (4.1)$$

where  $K_i$ ,  $\mu_i$  are the mean vector and co-variance matrix of the  $i$ th threat respectively and defined as  $\mu_i = \begin{bmatrix} \mu_{x,i} \\ \mu_{y,i} \end{bmatrix}$ , and  $K_i = \begin{bmatrix} \sigma_{x,i}^2 & 0 \\ 0 & \sigma_{y,i}^2 \end{bmatrix}$ .  $r$  is the position of a point of interest in a reference frame. In this research obstacles are assumed to be circular so  $\sigma_{x,i}^2 = \sigma_{y,i}^2$ .

## 4.2 PTEM Construction

### 4.2.1 Clustering of LaserRangeFinder Data

LRF provides a numerous data points for a single obstacle. The data points are clustered, in order for the PTEM to have a manageable size which makes the implementation computationally more efficient. The clustering of data points into a smaller subset is done based on a sequence of simple rules.

Clustering starts by considering very first data point as center of cluster with a predefined radius. The decision on whether to include a new point to an existing cluster see Fig. 4.1 or to create a new cluster is made based on its distance to the boundary of existing clusters. If the distance between the point of interest and the boundaries of existing clusters is greater than the threshold  $C_r$ , then a new individual cluster is created. The new cluster will be assigned a center as the point itself and radius equal to a predefined radius. If the new data point is close to an existing cluster (distance between the new data point and boundary of existing cluster is less than the  $C_r$ ), the cluster circle is updated to include the new point within the existing circle.

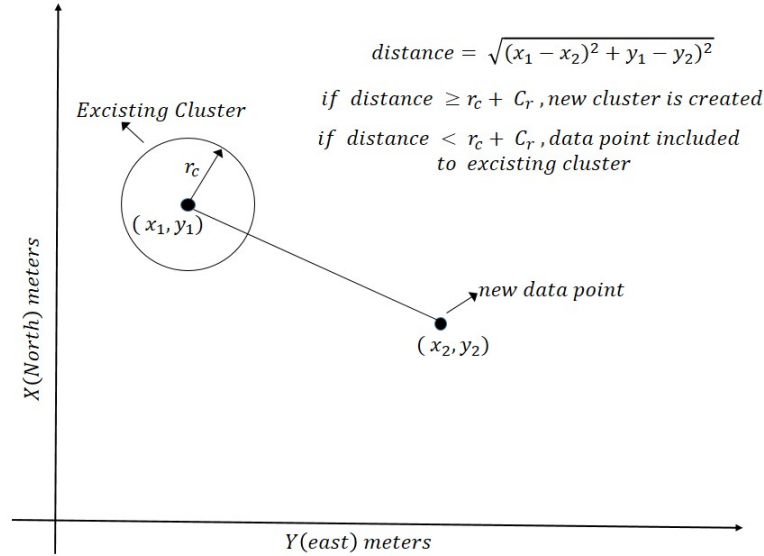


Figure 4.1. Clustering Data Points.

Once the new point is added to the cluster, a new circle is defined which encircles the current cluster circle and the new data point. The center and the radius of new circle is determined [5]. If the new data point is already inside the cluster, then no change is required. The threshold  $C_r$  in this research is equal to the width of the UGV because the UGV cannot go between two obstacles if the distance between them is less than the UGV width.

#### 4.2.2 Cumulative Clustering Algorithm

This PTEM construction algorithm is the prior method [5] developed under the assumption that obstacles are stationary. In this algorithm, the clusters created at the previous LRF scan are retained. The PTEM construction algorithm makes the assumption of stationary obstacles and thus treat the LRF readings as persistent obstacle information. As a result, PTEM circle (restricted region) grows bigger and

bigger when the obstacle happens to be moving. The cumulative clustering algorithm holds good for stationary obstacle but fails to handle the dynamic obstacles. Simulation and experimental results associated with this algorithm are discussed in Chapters 5 and 6.

#### 4.2.3 Single Scan Clustering Algorithm

This is the new PTEM construction method developed in this research. In this approach, the stationary obstacle assumption is removed and PTEM is updated continuously as new LRF reading are obtained. The data obtained from the previous scan of LRF is not retained. With this approach, the obstacle avoidance capability of UGV is enhanced to handle moving obstacle as well as the stationary obstacles. No change is needed in guidance algorithm since the PTEM will have representation of the obstacles at any given time. The new algorithm helps to overcome the problem associated with mobile obstacles. If the obstacle goes out of LRF scan area, the new approach retains the last seen information of obstacle. Simulation and experimental results of obstacle avoidance and waypoint navigation for moving as well as stationary obstacles with the new single scan algorithm are presented in Chapters 5 and 6. Single scan algorithm is explained in detail in the following subsections in terms of two example cases.

4.2.4 Case 1

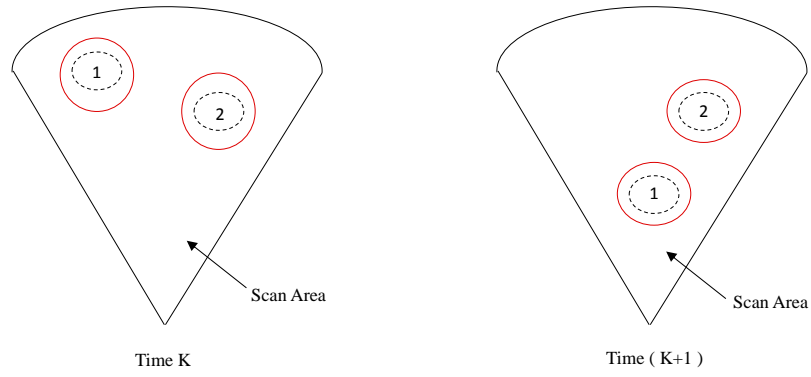


Figure 4.2. Single Scan Clustering Algorithm.

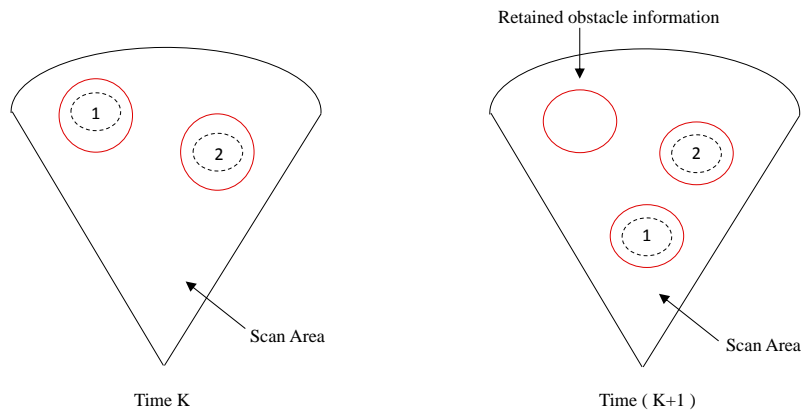


Figure 4.3. Cumulative Clustering Algorithm.

Let us consider that LRF scans an area that has two obstacles at sample time  $K$ . It is assumed that distance between the two obstacles are greater than the width of the vehicle. By the time of the next scan, one of the obstacle has moved to a new position as shown in the Fig. 4.2. If the LRF scans the same area at time  $(K+1)$  instant, the single scan approach algorithm updates the PTEM based on the new laser range finder readings obtained. Thus the updated PTEM construction will have representation of obstacle at any given time. On the other hand, the prior cumulative clustering algorithm retains the obstacle information as shown in Fig. 4.3 while it treats the obstacle at the new position as an additional obstacle and generate a new cluster for it. Circles in the figures with dotted lines represent obstacles.

#### 4.2.5 Case 2

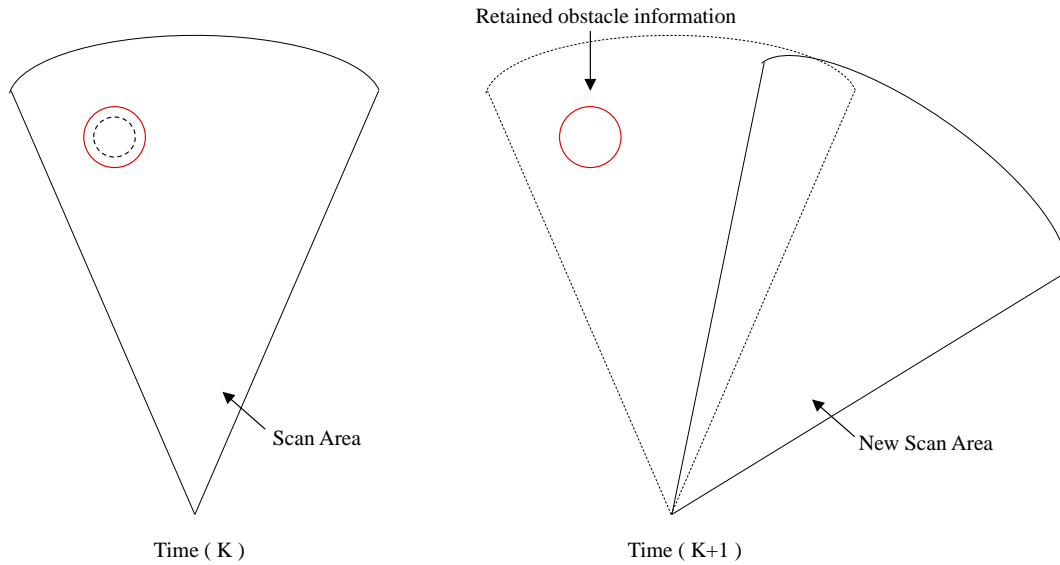


Figure 4.4. Single Scan Clustering Algorithm.

Fig. 4.4 shows an obstacle in LRF scan area at time interval K. It is represented as a restricted region (red circle) using Gaussian pdf. The obstacle is no longer in the scanning range of LRF at sample time (K+1), the single scan clustering algorithm retains information about the obstacle. All the previous information of obstacle is retained only if they fall outside the LRF limits whereas the previous algorithm used to retain it always.

### 4.3 Determining PTEM Variables

Once the clustering is performed, center and radius of each individual cluster is identified. For identifying the restricted areas within the PTEM, a threshold value,  $f_r$ , is needed. A threshold value is set by using the first cluster circle in

$$f(r) = \frac{1}{\sqrt{2\pi}\sigma} \exp\left[-\frac{r_{ca}^2}{2\sigma^2}\right] \quad (4.2)$$

where  $r_{ca}$  is the radius of first cluster and  $\sigma$  is variance pre-specified for the first cluster. Eq. (4.2) is obtained by substituting  $r=r_{ca}$  and  $\mu = 0$  in Eq. (4.1). The value of threshold calculated from the first cluster is fixed but is used for calculating the variances of the PDFs corresponding to all other clusters. The variance is calculated from Eq. (4.2) by solving for  $\sigma$ , given  $r_{ca}$  radius of the corresponding cluster circle and fixed threshold  $f_r$ . In this research the threshold is set to be 0.04 to accommodate sizes of obstacles considered in this research. Once the PTEM is constructed it is provided as input to the collision avoidance algorithm. The collision avoidance algorithm (Guidance Algorithm) determines in which direction and speed the UGV should move to avoid obstacles in its path and reach the desired waypoint.



#### 4.4 Virtual Target

The guidance algorithm used in this research was originally developed to track moving targets by keeping the host vehicle within the proximity of the target while avoiding restricted areas [30]. In this research, the UGV is tasked to go through set of waypoints while avoiding obstacles. To achieve waypoint navigation by the guidance algorithm, a virtual target is modeled to go through the assigned waypoints while the guidance algorithm moves the UGV to track the virtual target while avoiding the obstacles. Virtual target starts at the same position as UGV and moves with a constant speed in straight line connecting the waypoints. Virtual target does not consider the obstacles in the path. Once it reaches the waypoint, virtual target stops and waits for the UGV. A target proximity circle with a certain radius is defined to indicate how close the UGV should follow virtual target. Larger the target proximity circle UGV will follow the virtual target from the farther distance. For more information on virtual target, refer to [30].

#### 4.5 Guidance Algorithm

The guidance algorithm developed utilizing the concept of virtual target is adopted for obstacle avoidance and waypoint navigation of UGV. Gradient search approach [31] guidance algorithm determines in which direction the UGV should move to avoid entering restricted region or collision with obstacles. The main goal of the guidance strategy is to generate speed and heading angle commands to follow a moving virtual target in an area with obstacles. The highest priority of the strategy is to always avoid the restricted region. A safe heading range is which the directional derivative of the PTEM is zero or negative is determined. Trajectory of the virtual target is fed into the guidance algorithm which generates speed and heading

commands for the UGV. Guidance strategy is computationally feasible for configuring into an onboard micro-controller. The strategy has to take care of following objectives in the order of priorities:

1. Avoid all the obstacles or restricted regions.
2. UGV should maintain proximity with the moving virtual target.
3. Minimize the threat exposure level.

The guidance strategy computes the desired heading and speed in accordance to the three objectives mentioned above. At the same time, admissible or allowed speed and heading ranges are determined based on the PTEM and the dynamic constraints of the UGV. Then, the guidance strategy generates commanded heading and speed signals considering the desired heading and speed commands, and their respective admissible ranges. If the desired heading and speed are within the admissible range, then the desired signal is selected as a commanded signal. Otherwise, the allowed heading and speed closest to the desired signal is selected as the commanded signal. For more detailed information on how the guidance strategy is formulated, refer to [30].

## CHAPTER 5

### Stationary Obstacle Avoidance

This chapter presents the results of simulation and real time experiments for stationary obstacles. It presents a comparison between results obtained from cumulative approach (Old approach) and the new single scan approach. Experiments were carried out using circular obstacles of different sizes.

#### 5.1 Stationary Obstacle Avoidance Simulation Results

##### 5.1.1 Case 1

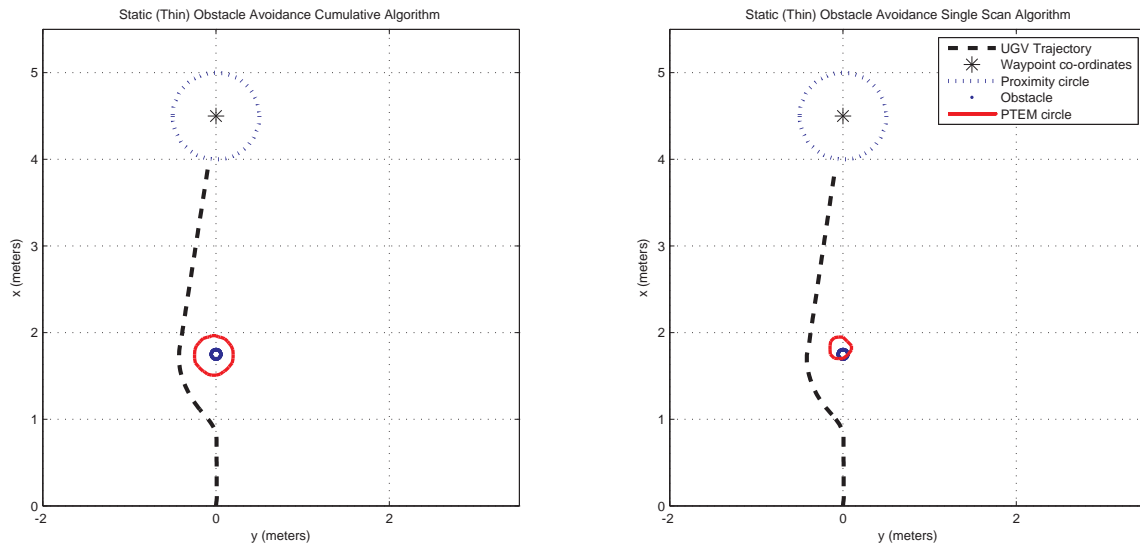


Figure 5.1. Trajectory of UGV avoiding thin stationary obstacle.

A thin circular obstacle of a radius 0.055 meters is placed at  $(x,y)= (1.75, 0)$ . Fig. 5.1 shows the trajectory of UGV successfully avoiding a thin stationary obstacle. It can also be seen from the Fig. 5.1 restricted region is bigger when using the Cumulative approach since we are retaining obstacle information obtained from the laser range finder after every scan. On the other hand in the single scan approach the PTEM is updated continuously as new LRF reading are obtained hence the restricted region is smaller. Single scan approach retains the last seen obstacle information.

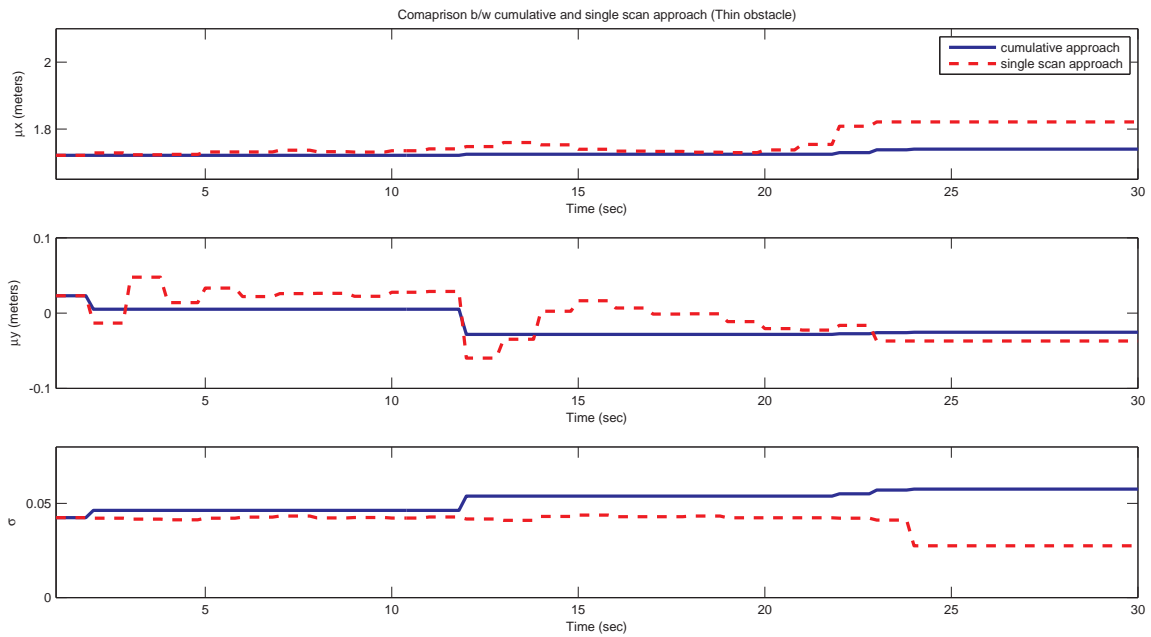


Figure 5.2. PTEM variables comparison b/w Cumulative and single scan approach for stationary obstacle Case 1.

Fig. 5.2 shows the time histories of mean values and variance of Gaussian PDF of the PTEM associated with the obstacle. It can be seen from Fig. 5.2 that the mean values almost remains constant for cumulative approach where as it varies in

single scan approach. Variance ( $\sigma$ ) value is high when using Cumulative approach which indicates the restricted region is bigger. This is because all the information coming from the LRF is retained in the cumulative approach.

### 5.1.2 Case 2

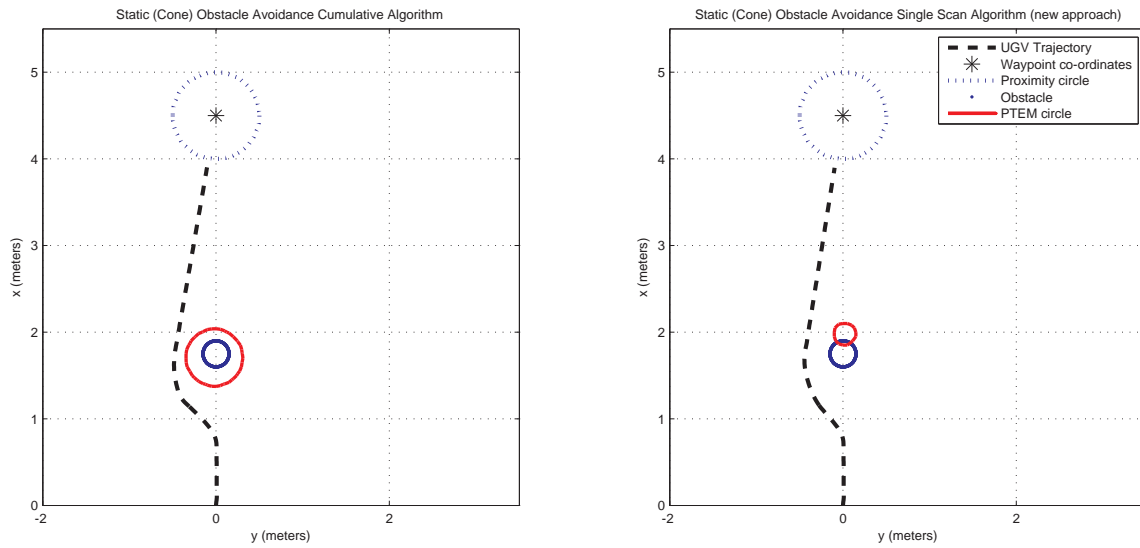


Figure 5.3. Trajectory of UGV avoiding stationary obstacle (Cone).

A stationary circular obstacle with a radius of 0.15 meters is placed at a distance of 1.75 meters north, ahead of the UGV starting position. Fig. 5.3 shows the trajectory of UGV successfully avoiding the stationary obstacle, using cumulative as well as the single scan clustering approach. For better understanding only the last value of the PTEM is plotted. The single scan approach retains the last seen position of the obstacle if obstacle goes beyond the LRF range.

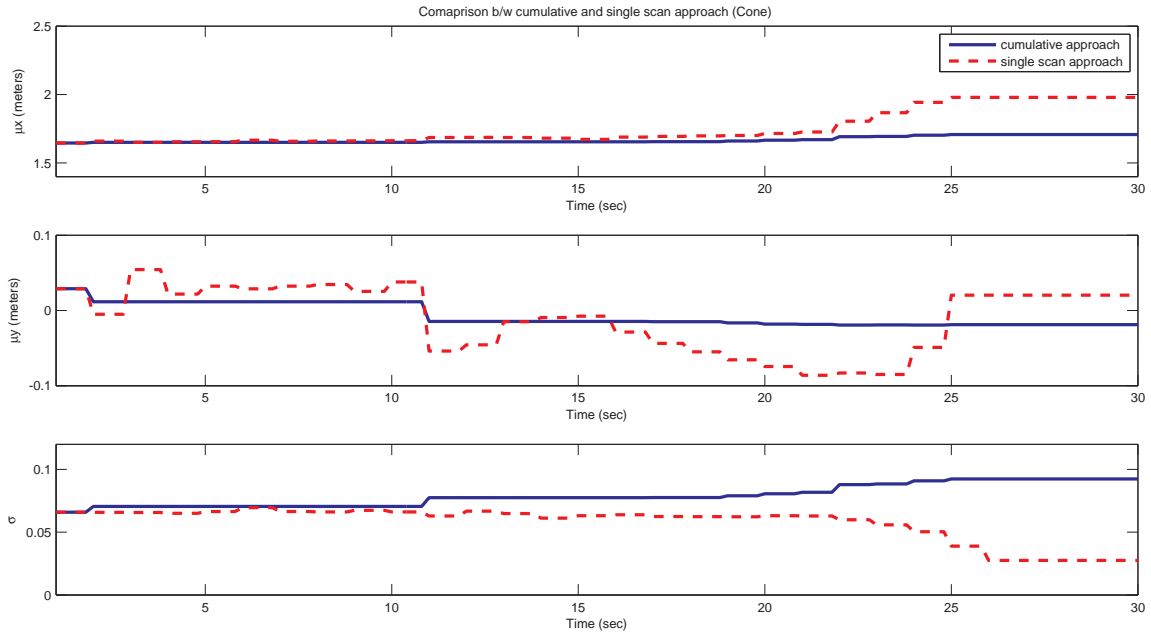


Figure 5.4. PTEM variables comparison b/w Cumulative and single scan approach for stationary obstacle Case 2.

Time series plots of mean and variance are given in Fig. 5.4 to show how the threat location and its area of influence vary with time. Since the obstacles are stationary there is not much variation in the mean values but still slight variations can be seen when using the new single scan clustering algorithm. Increase in variance value is attributed to the fact that cumulative clustering algorithm treats LRF readings as persistent information.

## 5.2 Stationary Obstacle Avoidance Experimental Results

Fig. 5.5 shows the the stationary obstacles used while conducting the real-time experiments in the lab environment. In the first case a thin circular obstacle was used whereas in the second case a cone was used.



(a) Thin obstacle



(b) Cone Obstacle

Figure 5.5. Stationary Obstacles.

5.2.1 Case 1

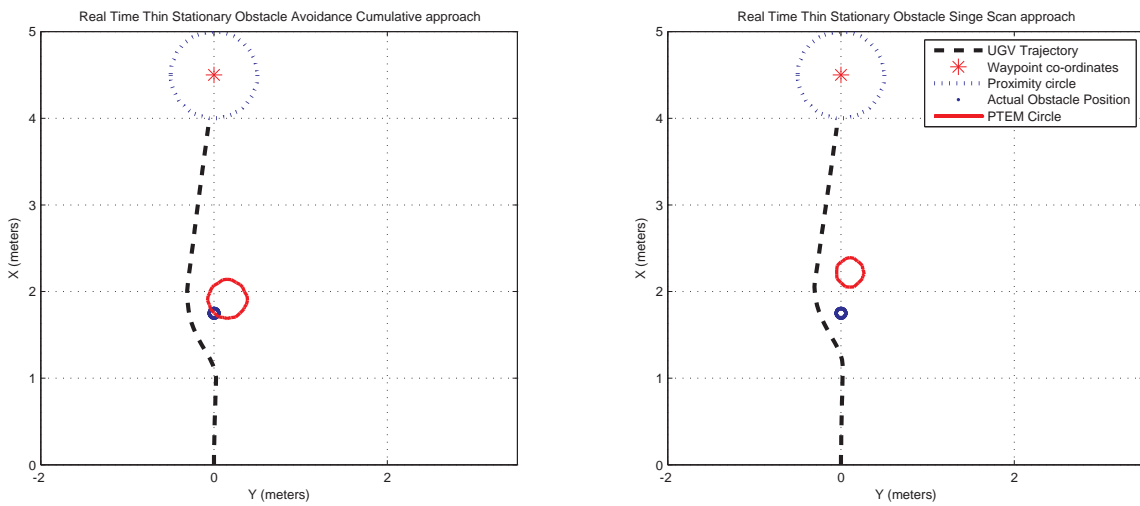


Figure 5.6. Real Time UGV Trajectory avoiding stationary thin obstacle.

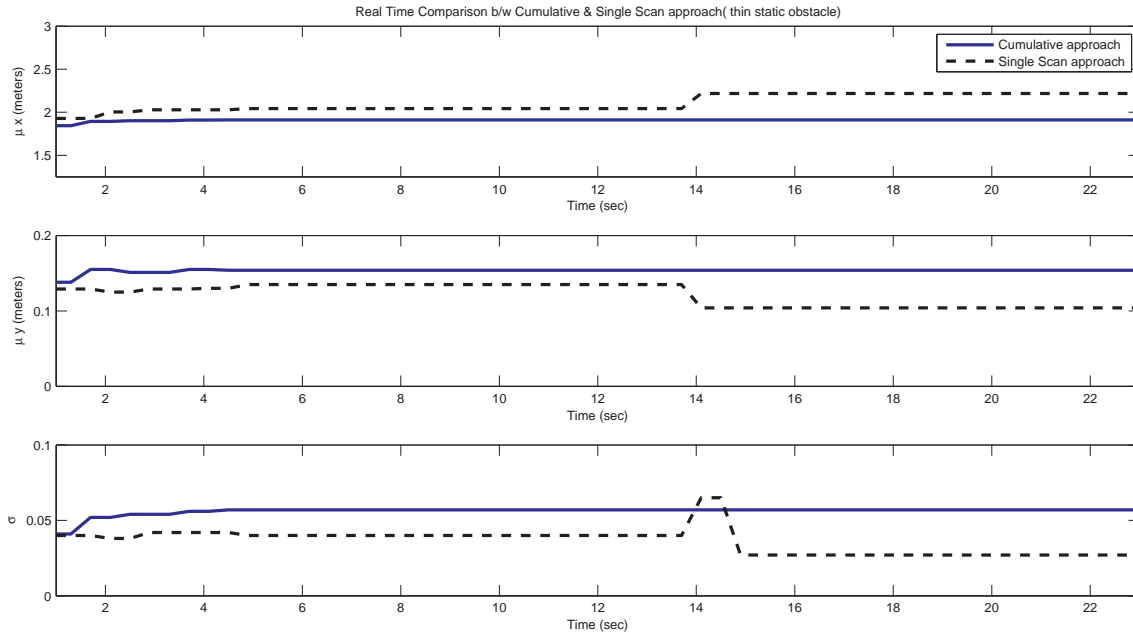


Figure 5.7. PTEM variables comparison b/w Cumulative and single scan approach for stationary obstacle Case 1.

Experiments were conducted in the lab environment to validate the new single scan clustering algorithm. Fig. 5.6 shows the UGV successfully avoiding the stationary obstacle placed at  $(x,y)=(1.75, 0)$ . The small blue circle indicates the actual obstacle position but in real time the LRF detects the obstacle at an offset. Some of the factors responsible for this offset are LRF reading (calibration error and accuracy), encoder readings. Position data of the ugv obtained from experimental runs are not the actual or measured positions of the UGV. They are estimated using a dead reckoning algorithm that uses the encoder counts from the left and the right wheels in estimating the position and orientation of the UGV. When there is slippage on the UGV tracks, the estimated position and the orientation will have errors. It should be noted that the PTEM circles are not the actual position of obstacle in real



time they just represent the restricted area. The PTEM circle is very small when using the single scan approach because only the last seen information of the obstacle is retained. Fig. 5.7 presents the times histories of mean position and variance of Gaussian PDF of PTEM associated with the obstacle. Mean values specify the obstacle locations whereas variance ( $\sigma$ ) represents the area of restricted region.

### 5.2.2 Case 2

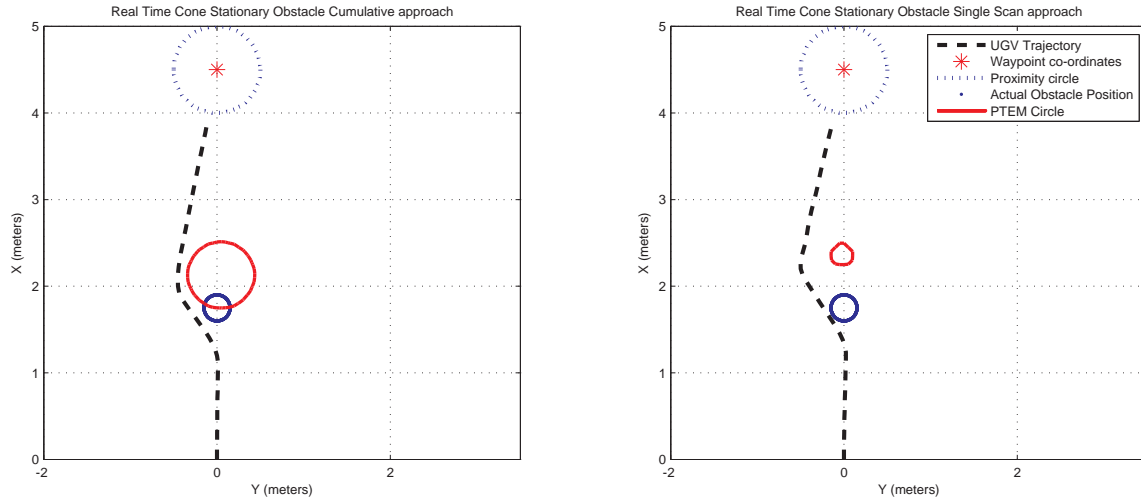


Figure 5.8. UGV Trajectory in Real Time avoiding stationary cone obstacle.

In this case a stationary circular obstacle with a radius of 0.15 m is placed at  $(x,y) = (1.75,0)$ . The restricted region is at a different location than the actual obstacle position. This is because PTEM is constructed based on the data obtained from LRF and encoders. The estimated position and orientation will have errors when there is slippage on the UGV tracks. Fig. 5.8 shows the trajectory of UGV successfully avoiding obstacle and navigating to the specified waypoint. Hence it can be concluded from the experimental results that the UGV successfully avoids the

stationary obstacle with the cumulative algorithm as well as with the new clustering algorithm.

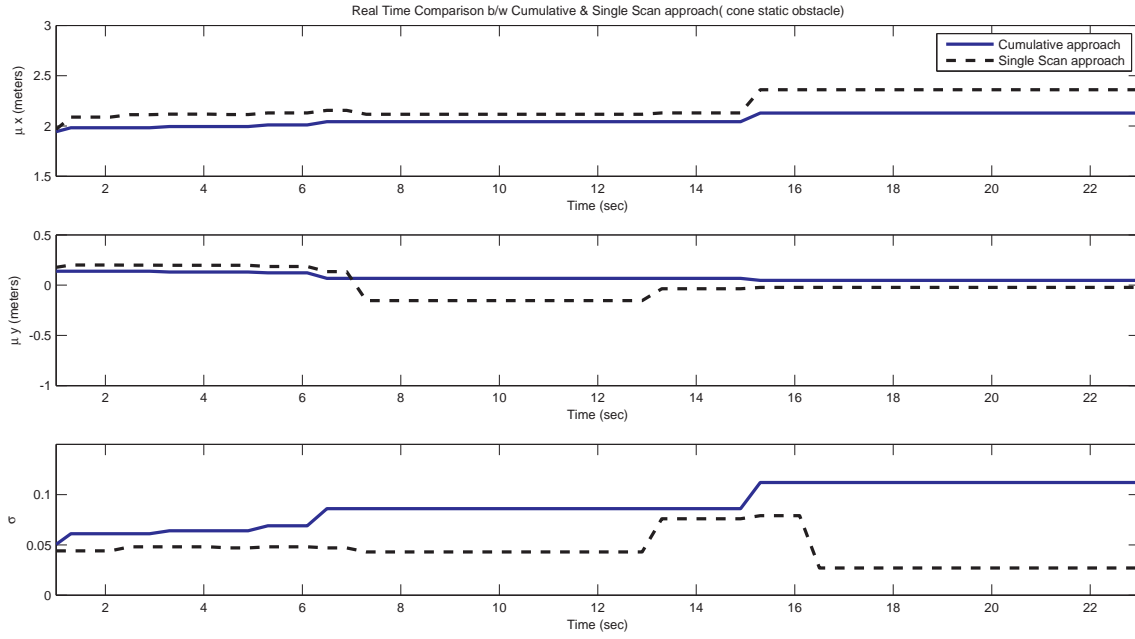


Figure 5.9. PTEM variables comparison b/w Cumulative and single scan approach for stationary obstacle Case 2.

Fig. 5.9 presents the times histories of mean position and variance ( $\sigma$ ) of Gaussian PDF of PTEM associated with the obstacle. It can be seen how the threat location and its area vary with respect to time. Some of the problems encountered while conducting the real time experiments are discussed at the end of Chapter 6.

## CHAPTER 6

### Dynamic Obstacle Avoidance

This chapter presents the simulation and experimental results for moving obstacle. Comparison is made between cumulative clustering approach and the new single scan clustering algorithm. It also shows how the new PTEM construction algorithm improves the performance in avoiding moving obstacles.

#### 6.1 Moving Obstacle Simulation Results

##### 6.1.1 Case 1

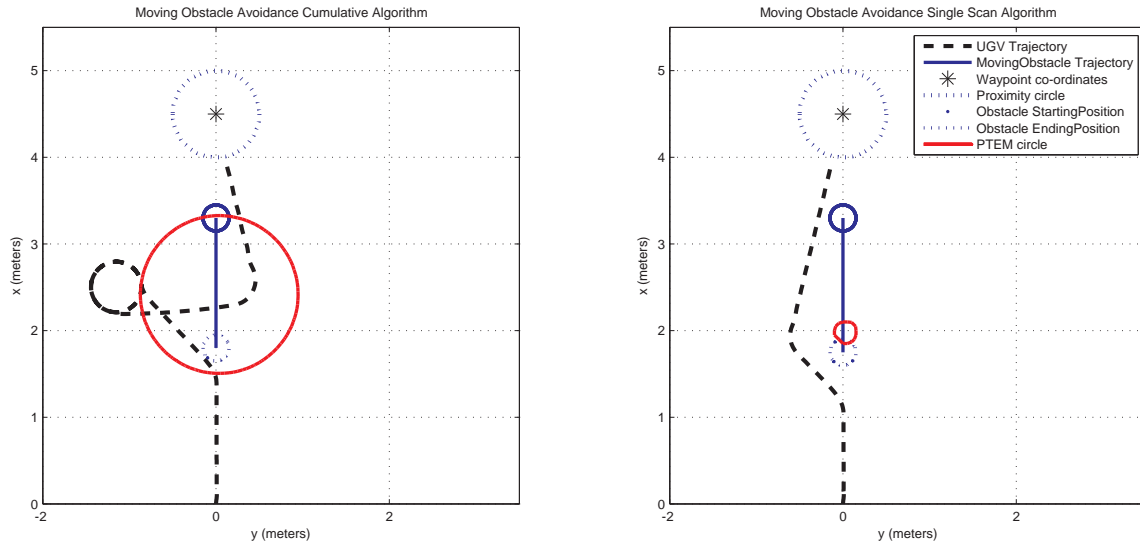


Figure 6.1. Trajectory of UGV for Moving obstacle.

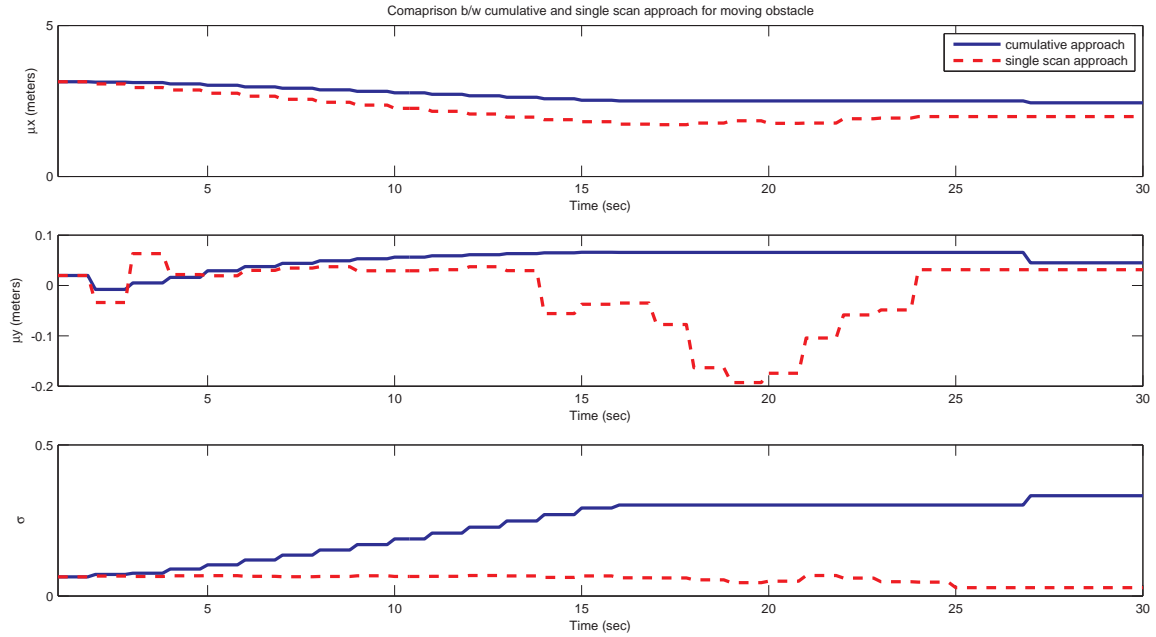


Figure 6.2. PTEM variables comparison b/w Cumulative and single scan approach for dynamic obstacle Case 1.

A dynamic obstacle with a constant velocity of 0.1 m/s is moving towards the UGV from its initial position  $(x,y)=(3.3, 0)$ . It can be seen from Fig. 6.1 the restricted region is huge by using cumulative clustering algorithm and as a result the UGV makes undesired maneuver to reach the specified waypoint. On the other hand new single scan clustering algorithm successfully avoids the dynamic obstacle coming in its way and reaches the specified waypoint. Only the last value of PTEM is shown in plots.

Fig. 6.2 shows how the obstacle locations (Mean values) of the PDF varies with time. Variance ( $\sigma$ ) increases with time which indicates restricted region is also getting bigger with time. This is due to cumulative clustering algorithm whereas in the new

clustering approach  $\sigma$  does not increase with time, since the PTEM construction will have representation of obstacle only at that instant.

### 6.1.2 Case 2

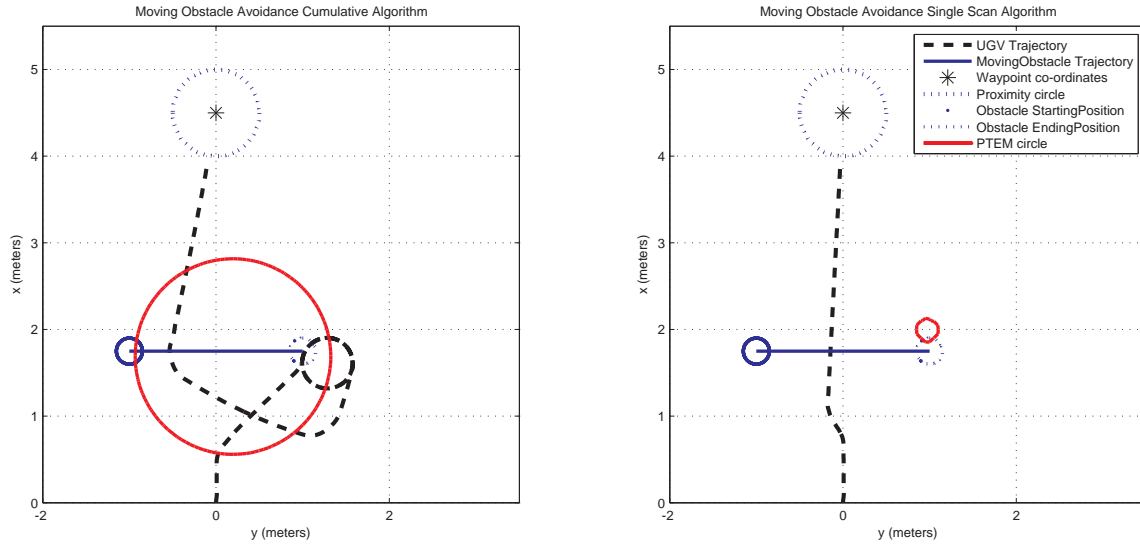


Figure 6.3. Trajectory of UGV for Moving obstacle.

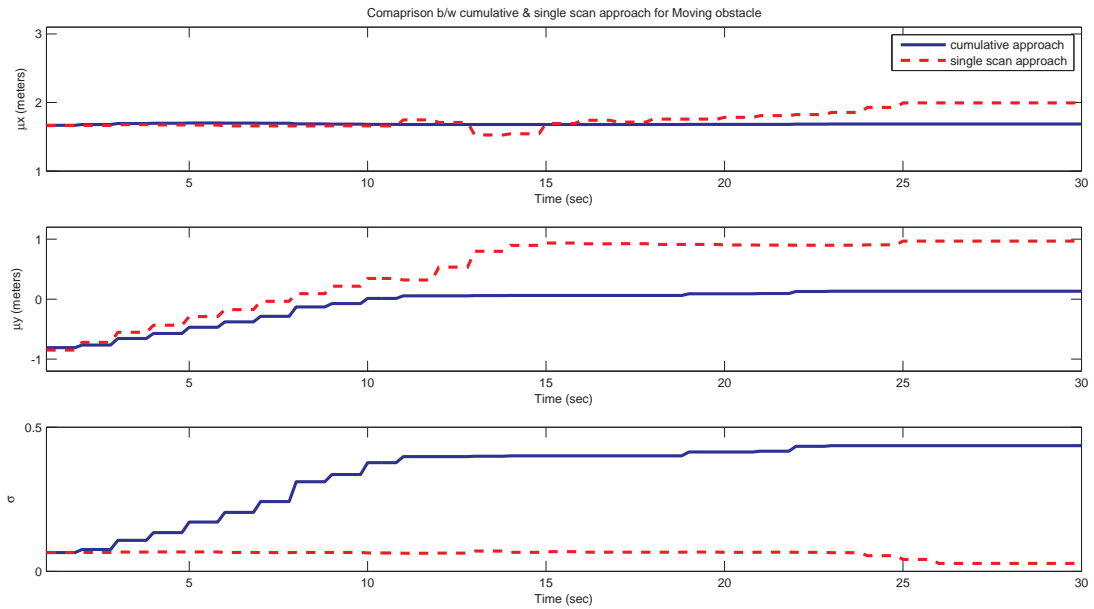


Figure 6.4. PTEM variables comparison b/w Cumulative and single scan approach for dynamic obstacle Case 2.

Dynamic Obstacle is placed at an initial position  $(x,y)=(1.75,-1)$  and moves transversely to UGV path with a velocity of 0.2 m/s to a new position  $(x,y)=(1.75,1)$ . It can be seen from Fig. 6.3 that the UGV navigates in an undesirable way to the specified waypoint because of the prohibitively large restricted area when the prior PTEM construction algorithm is used, whereas new clustering algorithm successfully avoids the moving obstacle.

Time series plots of the mean and variance are showed in Fig. 6.4 to provide information on locations of restricted area and it's influence. Variance increases with time when using cumulative approach, which indicates restricted area expanding with time.

## 6.2 Moving Obstacle Experimental Results

Real-time experiments were conducted in lab to validate the new single scan clustering algorithm for moving obstacles. The Cone was used as a moving obstacle instead of an actual moving circular platform. Fig. 6.5 shows the cone obstacle attached with a string and how the obstacle was moved during the experiment. The obstacle attached with a string was pulled towards the moving UGV to replicate the similar cases that were discussed in simulation environment.



(a) Cone obstacle with string



(b) Cone obstacle moved using string

Figure 6.5. Moving Obstacle.

### 6.2.1 Case 1

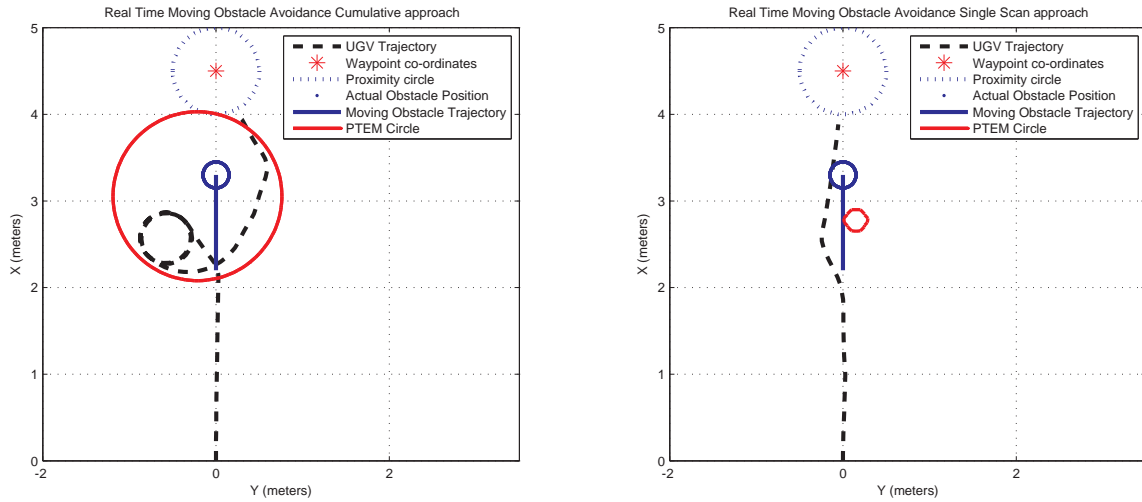


Figure 6.6. Trajectory of UGV .

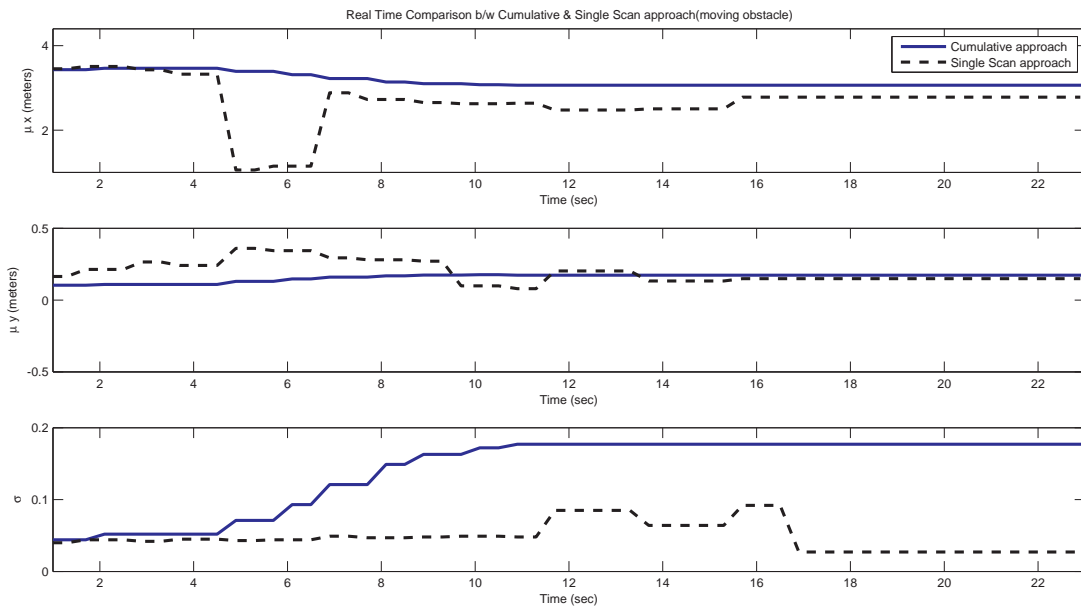


Figure 6.7. PTEM variables comparison b/w Cumulative and single scan approach for dynamic obstacle Case 1.



Initial position of the dynamic obstacle is at  $(x,y)=(3.3,0)$  and it is pulled towards the UGV. From Fig. 6.6 it can be seen that UGV performs undesired maneuver when using the cumulative clustering algorithm. The trajectory of the UGV is not the actual or measured positions of UGV, they are estimated by using the encoder ticks.

The real time run was repeated using the new single scan clustering algorithm where Fig. 6.6 shows a small PTEM unlike a very huge restricted region when using the cumulative clustering approach. The UGV successfully avoids the incoming obstacle and reaches the specified waypoint. Time history plots of the mean locations and variance ( $\sigma$ ) are given in Fig. 6.7 where it can be seen how the threat location and its area vary with respect to time. Variance increases with time when using cumulative approach, which indicates restricted area expanding with time. On the other hand in single scan approach the variance does not increase with time since the PTEM construction will have representation of obstacle only at that instant.

## 6.2.2 Case 2

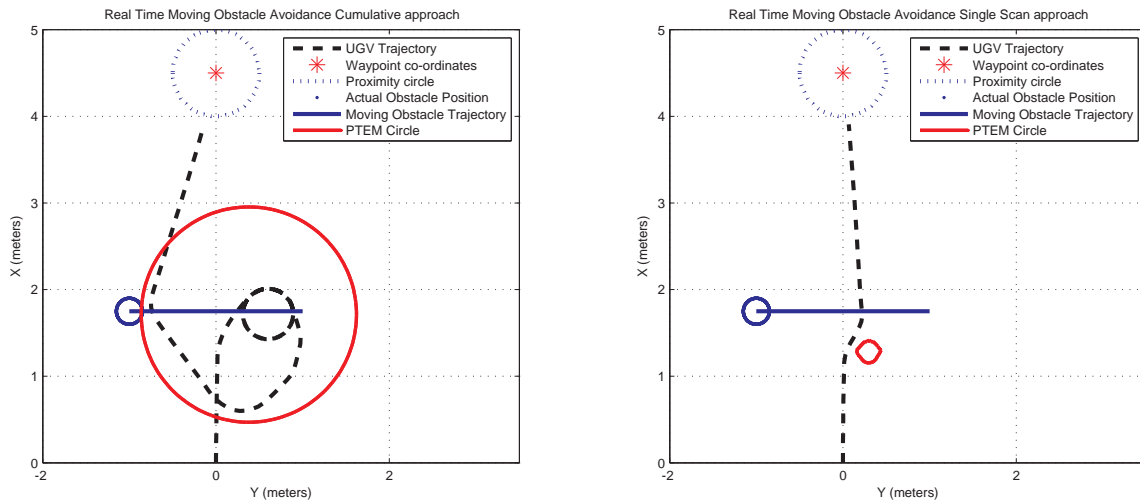


Figure 6.8. Trajectory of UGV .

In this case dynamic obstacle is moved in a transverse direction to UGV motion. Fig. 6.8 shows UGV performing undesirable motion when using the Cumulative clustering algorithm because of huge restricted area. The new single scan clustering algorithm constructs the PTEM on the most recent LRF scan hence the vehicle successfully navigates to the desired waypoint. Time history plots of the mean locations and variance ( $\sigma$ ) are given in Fig. 6.9 where it can be seen how the threat location and its area vary with respect to time.

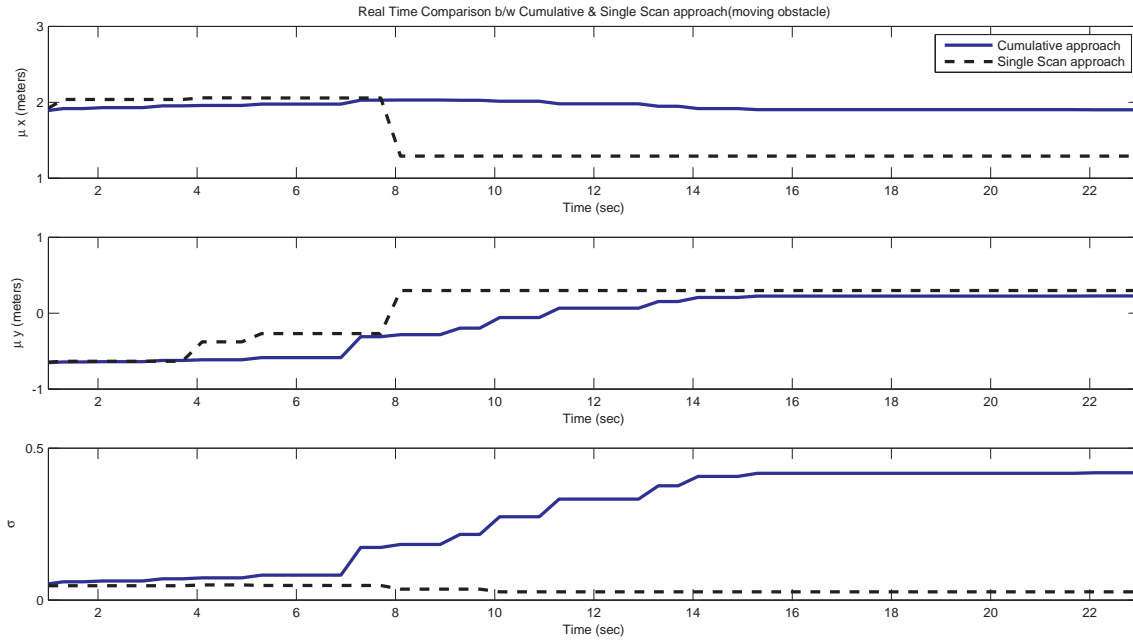


Figure 6.9. PTEM variables comparison b/w Cumulative and single scan approach for dynamic obstacle Case 2.

### 6.3 Problems Observed in Experiments

Real time experiments carried out using cumulative clustering approach as well as single scan approach gave some unexpected results. Some of the possible reasons and results are discussed below

#### 6.3.1 Observation 1

When the experiments were carried out using the cumulative PTEM algorithm for a stationary obstacle. It was noticed at times that the UGV directly hit the stationary obstacle placed in front of it instead of avoiding. It was observed that power to Plugapod was cut-off, which might be due to unreliable physical wiring and

also the LRF should be initialized properly. The same problem repeated when using the new single scan clustering approach.

### 6.3.2 Observation 2

The other observation made was that the UGV performs an undesirable loop when it tries to avoid a stationary obstacle from the right side. To understand this undesirable motion of UGV the experimental data was recorded and movie was made which shows the updated PTEM after every time step. It was seen as UGV tries to take a turn to avoid the obstacle the PTEM grows slightly bigger which makes the vehicle to go into a loop. The reason for this unsatisfactory PTEM construction has to be determined.

## CHAPTER 7

### Conclusion and Future Work

This chapter summarizes the research work and suggests what can be improved in the future research.

#### 7.1 Conclusion

First the problem associated with dynamic obstacles using the cumulative algorithm approach is introduced. Several cases using the cumulative approach were run in Matlab based simulation environment to see how the PTEM is constructed for dynamic obstacles. Two special cases in which the UGV enters into a loop was selected to show cumulative clustering algorithm needs modification to accommodate dynamic obstacles. A single scan clustering algorithm was developed. With this approach the PTEM was updated continuously as new LRF reading are obtained. The previous information is deleted so that the PTEM will have representation of obstacles at that instant. Using the Matlab/Simulink based simulation environment it was shown that dynamic obstacles were successfully avoided using single scan clustering algorithm. Experiments were carried out to see the effectiveness of new single scan clustering algorithm in realtime. Results were recorded which shows UGV avoiding both stationary and moving obstacles. However realtime experiments have to be repeated with actual moving platform to get consistent results. Some of the problems encountered while conducting the real-time experiments are discussed.

## 7.2 Future Work

Sensitivity of the UGV could be determined to get an idea how fast the UGV reacts to the incoming dynamic obstacles. The obstacles are assumed to be circular in shape. This can be extended to mobile obstacles of any shape. Hardware components used for realtime implementation can be made more reliable and robust to get consistent results. The LRF should be checked for accuracy and see if it requires calibration. PTEM construction algorithm can be extended for 3 dimension with the use of new 3D sensor. Multiple UGV's could be used in an area of operation and information can be shared between them. In this way, UGV's can obtain information about the obstacles even though they have not encountered an obstacle and their trajectories can be planned to avoid obstacles and reach the specified waypoint.

## REFERENCES

- [1] H. E. Sevil, P. Desai, A. Dogan, and B. Huff, “Real-time obstacle avoidance and waypoint navigation of an unmanned ground vehicle,” in *ASME 2012 5th Annual Dynamic Systems and Control Conference joint with the JSME 2012 11th Motion and Vibration Conference*. American Society of Mechanical Engineers, 2012, pp. 263–271.
- [2] R. Bishop, “Intelligent vehicle applications worldwide,” *Intelligent Systems and their Applications, IEEE*, vol. 15, no. 1, pp. 78–81, Jan 2000.
- [3] D. Glade, “Unmanned aerial vehicles: Implications for military operations,” DTIC Document, Tech. Rep., 2000.
- [4] S. Bhat and M. Meenakshi, “Vision based robotic system for military applications – design and real time validation,” in *Signal and Image Processing (ICSIP), 2014 Fifth International Conference on*, Jan 2014, pp. 20–25.
- [5] P. N. Desai, “Implementation of autonomous navigation and obstacle avoidance on an unmanned ground vehicle,” Master’s thesis, The University Of Texas at Arlington, Texas, United States, Dec 2009.
- [6] C.-H. Chen, C. Cheng, D. Page, A. Koschan, and M. Abidi, “A moving object tracked by a mobile robot with real-time obstacles avoidance capacity,” in *Pattern Recognition, 2006. ICPR 2006. 18th International Conference on*, vol. 3, 2006, pp. 1091–1094.
- [7] W.-J. Sohn and K.-S. Hong, “Moving obstacle avoidance using a lrf sensor,” in *SICE-ICASE, 2006. International Joint Conference*, Oct 2006, pp. 5957–5962.

- [8] L. Ren, W. Wang, and Z. Du, “On a laser rangefinder-based mobile robot obstacle avoidance strategy via local virtual target,” *Lasers in Engineering (Old City Publishing)*, vol. 25, 2013.
- [9] A. Typiak, “Use of laser rangefinder to detecting in surroundings of mobile robot the obstacles,” in *Symposium on Automation and Robotics in Construction*, 2008, pp. 26–29.
- [10] P. Moghadam, W. Wijesoma, and D. J. Feng, “Improving path planning and mapping based on stereo vision and lidar,” in *Control, Automation, Robotics and Vision, 2008. ICARCV 2008. 10th International Conference on*, Dec 2008, pp. 384–389.
- [11] S. Kodagoda, E. Hemachandra, P. G. Jayasekara, R. L. Peiris, A. De Silva, and R. Munasinghe, “Obstacle detection and map building with a rotating ultrasonic range sensor using bayesian combination,” in *Information and Automation, 2006. ICIA 2006. International Conference on*, Dec 2006, pp. 98–103.
- [12] K. Izumi, K. Watanabe, M. Shindo, and R. Sato, “A sensor fusion technique using visual and ultrasonic information to acquire obstacle avoidance behaviors for quadruped robots,” in *SICE-ICASE, 2006. International Joint Conference*, Oct 2006, pp. 5120–5125.
- [13] Q. Liu, Y. gang Lu, and C. xi Xie, “Optimal genetic fuzzy obstacle avoidance controller of autonomous mobile robot based on ultrasonic sensors,” in *Robotics and Biomimetics, 2006. ROBIO '06. IEEE International Conference on*, Dec 2006, pp. 125–129.
- [14] W. A. Lewinger, M. Watson, and R. Quinn, “Obstacle avoidance behavior for a biologically-inspired mobile robot using binaural ultrasonic sensors,” in *Intelligent Robots and Systems, 2006 IEEE/RSJ International Conference on*, Oct 2006, pp. 5769–5774.



- [15] J. Borenstein and Y. Koren, "Obstacle avoidance with ultrasonic sensors," *Robotics and Automation, IEEE Journal of*, vol. 4, no. 2, pp. 213–218, Apr 1988.
- [16] C.-H. Chao, B.-Y. Hsueh, M.-Y. Hsiao, S.-H. Tsai, and T. Li, "Real-time target tracking and obstacle avoidance for mobile robots using two cameras," in *ICCAS-SICE, 2009*, Aug 2009, pp. 4347–4352.
- [17] R. Lagisetty, N. Philip, R. Padhi, and M. Bhat, "Object detection and obstacle avoidance for mobile robot using stereo camera," in *Control Applications (CCA), 2013 IEEE International Conference on*, Aug 2013, pp. 605–610.
- [18] G. Spampinato, J. Lidholm, C. Ahlberg, F. Ekstrand, M. Ekstrom, and L. Asplund, "An embedded stereo vision module for industrial vehicles automation," in *Industrial Technology (ICIT), 2013 IEEE International Conference on*, Feb 2013, pp. 52–57.
- [19] A. Kosaka and A. Kak, "Fast vision-guided mobile robot navigation using model-based reasoning and prediction of uncertainties," in *Intelligent Robots and Systems, 1992., Proceedings of the 1992 IEEE/RSJ International Conference on*, vol. 3, Jul 1992, pp. 2177–2186.
- [20] O. Khatib, "Real-time obstacle avoidance for manipulators and mobile robots," in *Robotics and Automation. Proceedings. 1985 IEEE International Conference on*, vol. 2, Mar 1985, pp. 500–505.
- [21] D. Megherbi and V. Malayia, "Cooperation in a distributed hybrid potential-field/reinforcement learning multi-agents-based autonomous path planning in a dynamic time-varying unstructured environment," in *Cognitive Methods in Situation Awareness and Decision Support (CogSIMA), 2012 IEEE International Multi-Disciplinary Conference on*, March 2012, pp. 80–87.

- [22] Y. Koren and J. Borenstein, “Potential field methods and their inherent limitations for mobile robot navigation,” in *Robotics and Automation, 1991. Proceedings., 1991 IEEE International Conference on*, Apr 1991, pp. 1398–1404 vol.2.
- [23] H. Ishihara and E. Hashimoto, “Moving obstacle avoidance for the mobile robot using the probabilistic inference,” in *Mechatronics and Automation (ICMA), 2013 IEEE International Conference on*, Aug 2013, pp. 1771–1776.
- [24] W. Burgard, D. Fox, D. Hennig, and T. Schmidt, “Estimating the absolute position of a mobile robot using position probability grids,” in *Proceedings of the national conference on artificial intelligence*, 1996, pp. 896–901.
- [25] A. Dogan, “Probabilistic approach in path planning for uavs,” in *Intelligent Control. 2003 IEEE International Symposium on*, Oct 2003, pp. 608–613.
- [26] U. Zengin and A. Dogan, “Probabilistic trajectory planning for uavs in dynamic environments,” in *AIAA 3rd Unmanned Unlimited Technical Conference, Workshop and Exhibit, Chicago, IL*, 2004.
- [27] A. Fujimori and S. Tani, “A navigation of mobile robots with collision avoidance for moving obstacles,” in *Industrial Technology, 2002. IEEE ICIT '02. 2002 IEEE International Conference on*, vol. 1, 2002, pp. 1–6 vol.1.
- [28] T. Ishikawa, Y. Nishimura, and K. Hori, “Real-time collision avoidance in the environment with moving obstacles,” in *Computational Intelligence for Modelling Control Automation, 2008 International Conference on*, Dec 2008, pp. 569–574.
- [29] C.-H. Chao, B.-Y. Hsueh, M.-Y. Hsiao, S.-H. Tsai, and T. Li, “Real-time target tracking and obstacle avoidance for mobile robots using two cameras,” in *ICCAS-SICE, 2009*, Aug 2009, pp. 4347–4352.
- [30] U. Zengin, “Autonomous and cooperative multi-uav guidance in adversarial environment,” Ph.D. dissertation, The University Of Texas at Arlington, Texas, United States, May 2007.

- [31] U. Zengin and A. Dogan, “Real-time target tracking for autonomous uavs in adversarial environments: A gradient search algorithm,” in *Decision and Control, 2006 45th IEEE Conference on*, Dec 2006, pp. 697–702.

## BIOGRAPHICAL STATEMENT

Gangadhar Rajashekaraiah was born in Bangalore, Karnataka, India in 1990. He received his Bachelors in Mechanical Engineering from Reva Institute of Technology (a part of Visvesvaraiiah Technological University).He is currently pursuing his Master's in Mechcanical Engineering from University of Texas Arlington and his research is on implimentation of Moving obstacle detection and avoidance for Unmanned Ground Vehicle.